Adiabatic Passage to the Continuum: Controlling Ionization with Chirped Laser Pulses

Ulf Saalmann, Sajal Kumar Giri, and Jan M. Rost
Max-Planck-Institut für Physik komplexer Systeme, Nöthnitzer Str. 38, 01187 Dresden, Germany

(Received 4 July 2018; published 11 October 2018)

We demonstrate that, by changing the direction of the chirp in vacuum-ultraviolet pulses, one can switch between excitation and ionization with very high contrast, if the carrier frequency of the light is resonant with two bound states. This is a surprising consequence of rapid adiabatic passage if extended to include transitions to the continuum. The chirp phase locks the linear combination of the two resonantly coupled bound states whose ionization amplitudes interfere constructively or destructively depending on the chirp direction under suitable conditions. We derive the phenomenon in a minimal model and verify the effect with calculations for helium as a realistic example.

DOI: 10.1103/PhysRevLett.121.153203

Rapid adiabatic passage is an extremely simple, albeit rather efficient and robust, population-transfer technique. It has been known for a long time [1,2] and is explained in review papers [3–5] and textbooks [6]. Initially investigated for nuclear magnetic resonance [1], it was experimentally implemented with lasers for the first time in the 1970s (a list of experiments can be found in a review [3]). The necessary time-varying resonance condition was achieved by very different means: Stark shifts in molecules [7], chirping the laser frequency [8] position-dependent Doppler shift of the laser beam [9], or manipulating coupled waveguides [10]. The selected population of adiabatic states with chirped pulses has been measured *in situ* by weak-field ionization of the Stark-shifted states [11,12].

In the following we will demonstrate that in the context of intense vacuum-ultraviolet (VUV) pulses, a new possibility opens: namely to use the chirp *direction* as an effective control for turning ionization "on" or "off," although ionization is typically inevitable when atoms are exposed to VUV light. This is quite surprising since the direction of the chirp does not play any role in traditional rapid adiabatic passage [3–6]. Possible applications include suppression of ionization, an unavoidable but not always welcome effect of high-frequency laser-matter interaction. This is in particular true for coherent diffractive imaging [13], where ionization inflicts radiation damage. More generally, it may turn out that freely optimized pulses often contain chirped parts, which serve the purpose of transiently locking adiabatic states.

We will explain the main mechanism with a minimal model and show subsequently that our findings equally apply to real atoms. To this end we consider first an electron in one dimension subject to a soft-core Coulomb potential $V(x) = -1/\sqrt{x^2 + 1/2}$ and a Gaussian light pulse with the time-dependent vector potential

$$\mathcal{A}_\beta(t) = \mathcal{A}_\beta g_\beta(t) \cos(\phi_\beta(t)), \tag{1a}$$

$$g_\beta(t) = \exp(-2 \ln 2 t^2/T_\beta^2), \tag{1b}$$

whose frequency drifts linearly in time

$$\omega_\beta(t) = \frac{d}{dt}\phi_\beta(t) = \omega_0 + \frac{4 \ln 2}{\beta + 1/\beta}\frac{t}{T^2}, \tag{1c}$$

controlled by a dimensionless chirp parameter β. The Fourier-limited pulse ($\beta = 0$) is characterized by carrier frequency ω_0 and length T. Note, that the strongest chirp is achieved with $\beta = \pm 1$ and that any chirp stretches the pulse in time to $T_\beta = [1 + \beta^2]^{1/2} T$, which implies a reduced peak amplitude of $\mathcal{A}_\beta = [1 + \beta^2]^{-1/4} \mathcal{A}_{\max}$, leaving the pulse energy unchanged [14]. We solve the time-dependent Schrödinger equation (TDSE) including the light-matter coupling term $\mathcal{A}_\beta(t)\hat{p}$ in the basis of field-free eigenstates [[15], Sec. 2]. The two lowest states have energies of $E_0 = -24.2$ eV and $E_1 = -8.6$ eV, respectively, corresponding to a transition energy of $\Delta = E_1 - E_0 = 15.6$ eV. Although not essential, E_0 is close to the binding energy of helium.

The two-level system restricted to the two lowest states of the model, constitutes our case *I*. It shows upon driving with a chirped laser almost perfect rapid adiabatic passage, cf. Fig. 1(e). With a properly chosen carrier frequency, e. g., $\omega_0 = \Delta$ as in Fig. 1, the uncoupled dressed states with energies $E_0 + \omega_\beta(t)$ and E_1 would cross. The laser coupling, however, pushes them apart, as shown in Fig. 1(a), and thereby suppresses (nonadiabatic) transitions. As a consequence, only one adiabatic state is occupied for all times. Yet, this enables a transition since the adiabatic state changes its character [2–6]. The sign of the chirp β does not play any role. Indeed, the final occupation probability is identical for pulses "flipped" in time [[15], Sec. 4].

What happens if one bound state is replaced by a continuum allowing photoionization? We use the same underlying 1D system and laser parameters as before, but

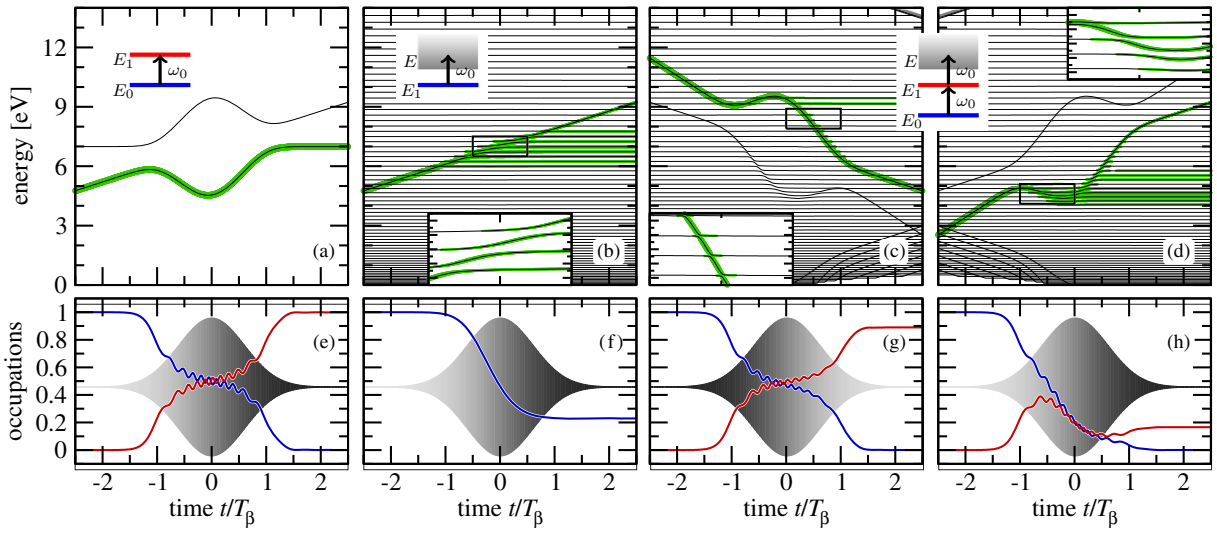

FIG. 1. Dressed-state description for cases *I*, *II*, and *III* as discussed in the text and sketched in the insets. Panels (a) and (e): two-level system with positively chirped pulse (case *I*). Panels (b) and (f): single level coupled to a continuum with positively chirped pulse (case *II*). Panels (c) and (g) and (d) and (h): two levels coupled to a continuum with negative and positive chirp, respectively (case *III*). Upper row: time-dependent energy levels (black lines) and corresponding occupations (green lines with the thickness corresponding to the occupation probability). The dense set of lines in (b)–(d) represents the discretized continuum. Lower row: occupation probability of the two lowest [in (f) only the lowest] field-free states. The gray-shaded areas show the envelope (with the brightness gradient illustrating the frequency chirp) of the driving laser pulse. Time t is measured in units of the pulse duration T_β.

remove the ground state and start from the first excited state, constituting case *II*. At a first glance, the dressed state with energy $E_1 + \omega_\beta(t)$ seems to intersect the levels of the discretized continuum, see Fig. 1(b). However, the diagonalized levels shown are adiabatic levels and exhibit narrow avoided crossings, facilitating nonadiabatic transitions, see the inset of Fig. 1(b). They form the most striking difference to the bound two-level system and allow us to preserve the initial state, if the level crossings are transversed diabatically. Nevertheless, the many possibilities to stay adiabatically in a continuum level lead to a significant depletion of the initial state. This is seen in Fig. 1(f), rendering the bound-continuum "two-level system" very similar to the bound-bound one, which is also corroborated by the fact that reversing the sign of the chirp does not change the depletion. Note, however, that with a reversed chirp, modified electron spectra may result in the saturation regime, since either the low-energy ($\beta < 0$) or the high-energy ($\beta > 0$) tail remains unpopulated.

In the next and final case *III*, we keep the continuum but again add the bound state, we had dropped before. Through the time-dependent frequency Eq. (1c) and the coupling, two adiabatic states are formed which contain roughly the same amount of the two bound states when the pulse is at full strength around $t = 0$, see Figs. 1(g) and 1(h). Yet, for this two-level system, which is in contrast to case *I* additionally coupled to the continuum, reversing the chirp has dramatic consequences: while the negative chirp leads to a similar effect as in the pure two-level system, namely a nearly complete exchange of the two bound states apart from small losses to the continuum [Fig. 1(c)], the system almost fully ionizes under positive chirp [Figs. 1(d) and 1(h)]. Note that for both chirp directions, the initial state gets fully depleted.

One can get from the insets of Figs. 1(c) and 1(d) a qualitative reason for this drastic difference: apparently the upper adiabatic state (referred to as "↑" in the following)—initially populated for the negative chirp—hardly couples to the continuum as apparent from the very narrow avoided crossings as the inset of Fig. 1(c) reveals. Comparatively broader avoided crossings [inset of Fig. 1(d)] indicate that the lower adiabatic state "↓", initially populated for the positive chirp exhibits a significant interaction with the continuum, similar to case *II* with one bound and one continuum state. As a consequence the ionization probability differs strongly when reversing the sign of the chirp parameter β. For negative β one sees hardly any ionization, for positive β there is strong ionization. We stress that the absolute value of the two pulses in the frequency domain is identical; they differ only by their phase. Hence, the difference in ionization cannot be attributed to a resonance effect: in fact, both pulses are resonant in the same manner. Also, for both chirp directions, the initial state gets fully depleted. One may say that the sign of the chirp decides if the three-level system behaves like the bound-bound (case *I*) or the bound-continuum (case *II*) system, although for each isolated two-level system the chirp direction does not matter.

Figure 2 summarizes the strong dependence of case *III* on the chirp, confirming that significant ionization occurs

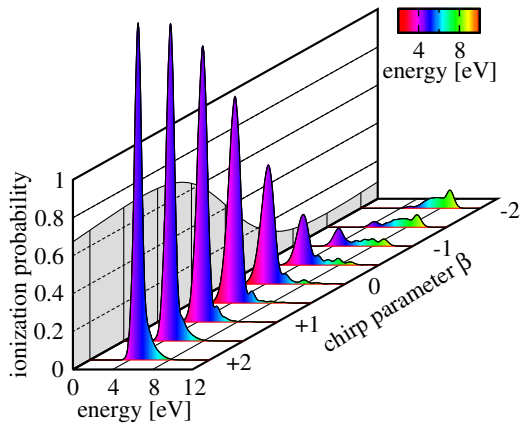

FIG. 2. Electron-energy spectra of the model system for various chirp parameters β. The pulse parameters [14] are $I = 3 \times 10^{15}$ W/cm^2, $T = 2$ fs, and $\omega_0 = 15.6$ eV. Without a Stark shift one would expect a peak at $E = 7$ eV. For negative β peaks shift towards higher energies, ionization is increasingly suppressed; this is most clearly seen from the integrated ionization probability shown as a gray-shaded area on the left side.

for $\beta > 0$ from the lower state "↓" since the peak energy is $E_{\text{peak}} \approx 4$ eV. On the other hand for $\beta < 0$, ionization originates from the upper state "↑" with $E_{\text{peak}} > 8$ eV but is strongly suppressed. Consequently, the total ionization yield (grey-shaded area) suddenly drops as a function of decreasing β around $\beta = 0$. The two peak positions result from an Autler-Townes splitting [18], from which we estimate at the maximal field strength $\mathcal{A}_\beta(t = 0) = \mathcal{A}_\beta$

$$E_{\downarrow\uparrow} = E_0 + 2\omega_0 \mp \Omega_{01}, \tag{2}$$

with the laser frequency $\omega_\beta(t = 0) = \omega_0 = \Delta$, cf. Eq. (1c), and the Rabi frequency $\Omega_{01} \equiv \frac{1}{2}|\mathcal{A}_\beta V_{01}|$, where $V_{jj'}$ denotes the coupling matrix element. We obtain $E_\downarrow = 3.6$ eV and $E_\uparrow = 10.4$ eV for the parameters of Fig. 2 in good agreement with the peak positions seen there.

Why does a typical two-level adiabatic passage system become extremely sensitive to the chirp direction when coupled to a continuum? An essential dressed-state representation, where the Hamilton matrix is augmented with states "dressed" by an appropriate number of photons, provides the answer. Summarizing the detailed derivation in the Supplemental Material [[15], Sec. 3], the minimal states required are the two bound states φ_0 and φ_1, resonantly coupled through V_{01} with $E_1 - E_0 = \omega_0$ and two states φ_u and φ_g in the continuum with the same energy E but different symmetry. The latter couple among each other through V_{ug} and each of them couples to one bound state via the matrix elements V_{0u} and V_{1g}, respectively. In the dressed-state representation, states couple only if they have opposite symmetry (gerade vs ungerade) and if they differ by exactly one dressing photon. Therefore, the effective Hamiltonian matrix constructed from the four states contains only five dressed states and can be cast into a form where the 2×2 bound and the 3×3 continuum blocks are diagonalized [15]:

$$\left(\begin{array}{cc|ccc} E_0 + 2\omega & \Omega_{01} & \Omega_{0u} & 0 & 0 \\ \Omega_{10} & E_1 + \omega & 0 & \Omega_{1g} & 0 \\ \hline \Omega_{u0} & 0 & E + \omega & \Omega_{ug} & 0 \\ 0 & \Omega_{g1} & \Omega_{gu} & E & \Omega_{gu} \\ 0 & 0 & 0 & \Omega_{ug} & E - \omega \end{array}\right)$$

$$\rightarrow \left(\begin{array}{cc|ccc} E_\downarrow & 0 & \cdot & C_\downarrow & \cdot \\ 0 & E_\uparrow & \cdot & C_\uparrow & \cdot \\ \hline \cdot & \cdot & \cdot & 0 & \cdot \\ C_\downarrow & C_\uparrow & 0 & E & 0 \\ \cdot & \cdot & \cdot & 0 & \cdot \end{array}\right).$$

Here, ω denotes the instantaneous frequency $\omega_\beta(t)$ and the Rabi frequencies are defined as $\Omega_{jj'} \equiv \frac{1}{2}\mathcal{A}_\beta g_\beta(t) V_{jj'}$ with g_β the Gaussian from Eq. (1b). We would like to stress that the chirp β merely selects the adiabatic state, "↓" vs "↑", but is not essential for the subsequent discussion. The coupling terms $C_{\downarrow\uparrow}$ read for the case $E_0 + \omega = E_1$ as

$$C_{\downarrow\uparrow} = \frac{\mp\,\Omega_{0u}\Omega_{ug} - \omega\Omega_{1g}}{\sqrt{2\omega^2 + 4\Omega_{ug}^2}}. \tag{3}$$

At the pulse peak, the coupling $C_\uparrow$ vanishes for

$$\frac{\Omega_{0u}}{\Omega_{1g}} = \frac{\omega}{\Omega_{ug}} \quad \text{or} \quad \frac{\mathcal{A}_\beta}{2}\frac{V_{0u}}{V_{1g}} = \frac{\omega_0}{V_{ug}}. \tag{4}$$

Together with the adiabatic locking to either state "↓" or "↑" (i.e., keeping a fixed combination of ground and excited state, just as in conventional rapid adiabatic passage) this explains the very different electron dynamics for positive or negative chirps β, respectively. That the chirp with direction $\text{sgn}(\beta) = \pm 1$ creates a locked linear combination in time is illustrated in Figs. 3(a) and 3(b) with the time-dependent bound-state density in the model, which oscillates with the energy difference $\omega_0 = E_1 - E_0$ of the bound states but is otherwise stationary over the main part of the pulse.

Having established that the chirp generates a locked linear combination of the two bound states even in the presence of the continuum (and possibly other bound states), it is tempting to describe adiabatic passage to the continuum as a standard strong-field ionization process [19]

$$|\psi(t)\rangle = -i \int^t dt' \hat{U}(t, t') \mathcal{A}_\beta(t') \hat{p} |\psi_{\text{ini}}(t')\rangle, \tag{5a}$$

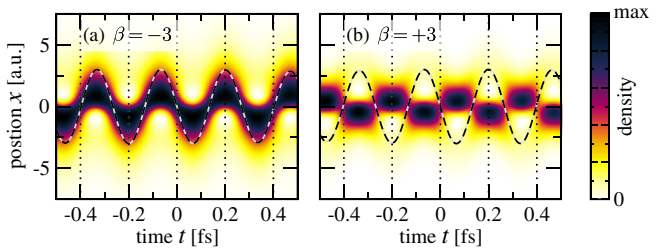

FIG. 3. Oscillating density for negative (a) and positive (b) chirp, respectively. The densities are obtained by solving the TDSE for the 1D model system ($I = 3 \times 10^{15}$ W/cm^2, $T = 1$ fs, $\omega_0 = 15.6$ eV [14]). The different phase lag of the oscillations with respect to the laser's electric field (dashed lines) is due to the different combination of ground and excited state in either the "↑" (a) or "↓" (b) adiabatic state, respectively. Note that the difference in chirp is invisible.

with the initial "chirp-locked" state

$$|\psi_{\rm ini}(t')\rangle = {\rm sgn}(\beta)|0\rangle e^{-iE_0 t'} + |1\rangle e^{-iE_1 t'}, \qquad (5b)$$

and the (Volkov) propagator

$$\hat{U}(t,t') = e^{-i\int_{t'}^{t} dt''[\hat{p}^2/2 + \hat{p}A_\beta \cos(\omega_0 t'')]}. \qquad (5c)$$

For the latter we fix the vector potential at maximal field strength A_β and neglect the chirp in the frequency since it changes the photon energy maximally by $|\delta\omega/\omega_0| < 0.03$ for our parameters.

With these approximations, we can use Eq. (5) in order to calculate the amplitude $\langle k|\psi(t)\rangle$ for a specific continuum state with momentum k analytically [15]. At resonance $k^2/2 = E_0 + 2\omega_0 = E_1 + \omega_0$ and in leading order of the electron-photon coupling parameter

$$\lambda = A_\beta k/\omega_0, \qquad (6)$$

the ionization probability $P_{\rm ion}^{\rm res} \equiv |\langle k|\psi(t\to\infty)\rangle|^2$ reads

$$P_{\rm ion}^{\rm res} \propto |{\rm sgn}(\beta)\langle k|0\rangle\lambda^2/2 + \langle k|1\rangle\lambda|^2. \qquad (7)$$

Obviously, ionization is suppressed for a negative chirp $\beta < 0$ if $\langle k|0\rangle\lambda/2 = \langle k|1\rangle$. It can be shown [15] that this condition is equivalent to condition in Eq. (4) above. Moreover, $P_{\rm ion}^{\rm res}$ clearly shows that the suppression or enhancement of ionization in the dressed continuum, dependent on the chirp direction, is due to destructive or constructive interference of the lower bound state $|0\rangle$ having absorbed two photons ($\propto \lambda^2$) and the higher bound state $|1\rangle$ after absorption of one photon ($\propto \lambda$).

Having worked out adiabatic passage to the continuum with a minimal model, we will finally demonstrate it for realistic 3D systems, whereby $\vec{\mathcal{A}}_\beta(t) = \mathcal{A}_\beta(t)\vec{e}_z$. To this end we will present calculations for a helium atom within the single-active-electron approximation, certainly applicable for the parameters used. With technical details summarized

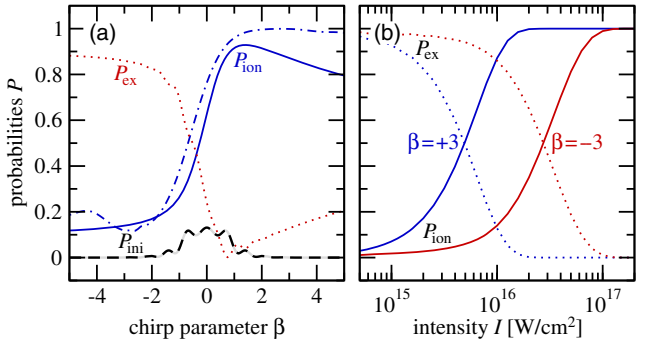

FIG. 4. Ionization ($P_{\rm ion}$, solid) and excitation ($P_{\rm ex}$, dotted) probabilities for helium as a function of the chirp β (a) and as a function of the laser intensity I (b). The pulse [14] has an intensity of $I = 10^{16}$ W/cm^2 (a) and a length of $T = 3$ fs (a) and (b). In panel (a) we also show the probability for remaining in the initial state ($P_{\rm ini}$, dashed) and the ionization probability for the 1D model system (dot-dashed) discussed in the text.

in the Supplemental Material [15], we show results in Figs. 4 and 5. As before, all calculations are done for the resonant frequency $\omega_0 = \Delta = E_{2p} - E_{1s} \approx 21$ eV, but apply similarly to quasi-resonant frequencies ω_0.

Figure 4(a) shows a clear transition of the ionization probability $P_{\rm ion}$ as a function of the chirp β with a contrast of about 80%. Closely related, and almost complementary to this behavior, the excitation probability $P_{\rm ex}$ changes. For chirp values $|\beta| > 2$ these two quantities add up approximately to 1. For smaller β the initial $1s$ state does not get fully depleted, cf. dashed line in Fig. 4(a). The symmetry

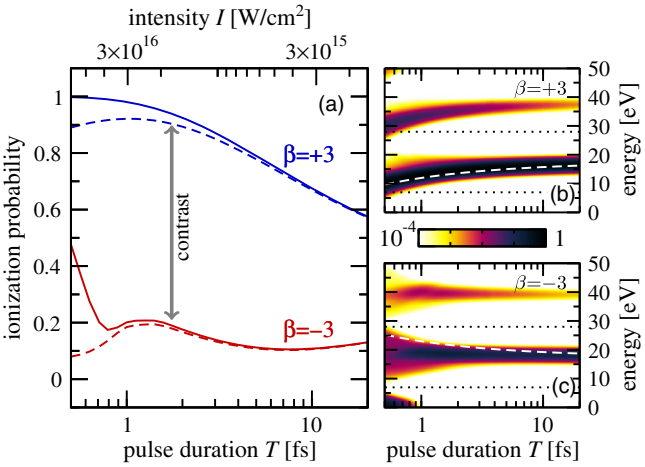

FIG. 5. Ionization probabilities (a) and photoelectron spectra (b) and (c) as a function of pulse duration T for two chirp parameters $\beta = \pm 3$. The pulse energy is kept constant such that $I \times T = 3 \times 10^{16}$ W fs/cm^2. The dashed lines show the ionization probability with final electron energy E in the "two-photon region" $E_0 + 3\omega_0/2 \le E \le E_0 + 5\omega_0/2$. This energy interval is marked by dotted lines in the pulse-dependent electron spectra (b) and (c). The white dashed lines mark the expected spectral peaks from the Autler-Townes splitting of the two ↑↓ states as given in Eq. (2).

$P_{\mathrm{ini}}(-\beta) = P_{\mathrm{ini}}(+\beta)$ follows from a more general relation for pulses "flipped" in time [15]. Figure 4(b) shows the ionization (and for completeness the excitation) probability as a function of laser intensity I for two chirp parameters $\beta = \pm 3$ and fixed pulse duration of $T = 3$ fs [14]. The graph covers the entire range from negligible ionization to full saturation. Note, that this transition occurs at rather different intensities for positive and negative chirps β.

Finally, Fig. 5 confirms the important role of two-photon absorption for the chirp-sensitive ionization according to Eq. (7): long pulses are too weak (note that we use fixed-fluence pulses in Fig. 5) for efficient two-photon processes such that the condition for perfect interference is missed by an increasing margin lowering the contrast of negative and positive chirped ionization. Short pulses weaken the prevalence of the resonant energy k due to their large energy spread and the fact that also higher-order multiphoton processes can be realized due to the large intensity of the light. This is indicated by the larger deviation between full ionization and ionization by two photons (dashed lines) for short pulses. Moreover, ultrashort pulses activate the qualitatively different regime of nonadiabatic photoionization [20].

To summarize: if rapid adiabatic passage is extended to include transitions to the continuum, the direction of the chirp decides if ionization is suppressed in favor of excitation with high contrast or vice versa. The phenomenon is universal for suitable combinations of parameters which occur naturally, e.g., for intense VUV pulses exciting resonantly the $1s$-$2p$ transition in helium. It is remarkable that the locking of the bound states due to the chirp persists during the main part of the pulse almost unaffected by the laser-induced interaction with free electrons which act as an ordinary photon-dressed continuum. This may in general simplify in the future the approach to electron dynamics controlled by shaped light pulses.

One of us (US) gratefully acknowledges a lively discussion with A. Emmanouilidou, R. Moshammer, T. Pfeifer, and A. Saenz during an "Atomic Physics Work-shop" in Dresden. This work has been supported by the Deutsche Forschungsgemeinschaft (DFG) through the priority program 1840 "Quantum Dynamics in Tailored Intense Fields."

[1] F. Bloch, Phys. Rev. **70**, 460 (1946).
[2] V. S. Malinovsky and J. L. Krause, Eur. Phys. J. D **14**, 147 (2001).
[3] N. V. Vitanov, T. Halfmann, B. W. Shore, and K. Bergmann, Annu. Rev. Phys. Chem. **52**, 763 (2001).
[4] D. Goswami, Phys. Rep. **374**, 385 (2003).
[5] H. Metcalf, Rev. Mod. Phys. **89**, 041001 (2017).
[6] B. W. Shore, *Manipulating quantum structures using laser pulses* (Cambridge University Press, Cambridge, 2011).
[7] M. M. T. Loy, Phys. Rev. Lett. **32**, 814 (1974).
[8] S. M. Hamadani, A. T. Mattick, N. A. Kurnit, and A. Javan, Appl. Phys. Lett. **27**, 21 (1975).
[9] J. P. C. Kroon, H. A. J. Senhorst, H. C. W. Beijerinck, B. J. Verhaar, and N. F. Verster, Phys. Rev. A **31**, 3724 (1985).
[10] H. Oukraou, L. Vittadello, V. Coda, C. Ciret, M. Alonzo, A. A. Rangelov, N. V. Vitanov, and G. Montemezzani, Phys. Rev. A **95**, 023811 (2017).
[11] M. Wollenhaupt, A. Präkelt, C. Sarpe-Tudoran, D. Liese, and T. Baumert, Appl. Phys. B **82**, 183 (2006).
[12] M. Krug, T. Bayer, M. Wollenhaupt, C. Sarpe-Tudoran, T. Baumert, S. S. Ivanov, and N. V. Vitanov, New J. Phys. **11**, 105051 (2009).
[13] H. N. Chapman, C. Caleman, and N. Timneanu, Phil. Trans. R. Soc. B **369**, 20130313 (2014).
[14] Specific values of pulse duration T and intensity I in the text always refer to the Fourier-limited (i.e., chirp-free) pulse.
[15] See Supplemental Material at http://link.aps.org/supplemental/10.1103/PhysRevLett.121.153203, which contains additional references [16,17].
[16] M. Wollenhaupt, A. Assion, and Th. Baumert, in *Springer Handbook of Lasers and Optics*, edited by F. Träger (Springer, Berlin, Heidelberg, 2012).
[17] X. M. Tong and C. D. Lin, J. Phys. B **38**, 2593 (2005).
[18] S. H. Autler and C. H. Townes, Phys. Rev. **100**, 703 (1955).
[19] F. Quéré, Y. Mairesse, and J. Itatani, J. Mod. Opt. **52**, 339 (2005).
[20] Q.-C. Ning, U. Saalmann, and J. M. Rost, Phys. Rev. Lett. **120**, 033203 (2018).

Supplement "Adiabatic passage to the continuum"

Ulf Saalmann, Sajal Kumar Giri, and Jan M. Rost

Technical details for laser pulses and the treatment of the time-dependent Schrödinger equation, with all of them being standard, are provided. Parameters for the numerical calculations are specified. Furthermore, we give details for deriving the conditions for ionization suppression. Finally, a proof for pulses "flipped" in time is given.

1 Chirped laser pulses

We consider only Gaussian pulses

$$\mathcal{A}_\beta(t) = \mathcal{A}_\beta\, g_\beta(t) \cos\big(\phi_\beta(t)\big) \quad \text{with the envelope} \quad g_\beta(t) = \mathrm{e}^{-2\ln 2\, t^2/T_\beta^2}, \tag{S1a}$$

$\mathcal{A}_\beta$ being the peak value of the vector potential and T_β the full-width-at-half-maximum pulse duration. By means of a quadratic modification of the phase in the frequency domain around the central frequency ω_0

$$\widetilde{\phi}_\beta(\omega) = \beta \frac{T^2}{4\ln 2}[\omega-\omega_0]^2, \tag{S1b}$$

the phase in time in Eq. (S1a) grows also quadratically [1]

$$\phi_\beta(t) = \omega_0 t + \frac{\chi_\beta}{2}\frac{t^2}{T^2} \quad \text{with the pre-factor} \quad \chi_\beta \equiv \frac{4\ln 2}{\beta+1/\beta}. \tag{S1c}$$

This results in a linear chirp of the instantaneous frequency $\omega_\beta(t) = \frac{\mathrm{d}}{\mathrm{d}t}\phi_\beta(t)$

$$\omega_\beta(t) = \omega_0 + \chi_\beta \frac{t}{T^2}. \tag{S1d}$$

The rate of frequency change is $\frac{\mathrm{d}}{\mathrm{d}t}\omega_\beta(t) = \chi_\beta/T^2$, which becomes largest for a given pulse duration T where the prefactor χ_β is maximal. This occurs for $\beta = \pm 1$, with $\frac{\mathrm{d}}{\mathrm{d}t}\omega_{\beta=\pm1} = \pm 2\ln 2/T^2$. Note that a finite chirp β modifies the effective strength and pulse duration in the envelope function (S1a) according to

$$\mathcal{A}_\beta = \frac{\mathcal{A}_{\max}}{\sqrt[4]{1+\beta^2}} \quad \text{and} \quad T_\beta = \sqrt{1+\beta^2}\, T. \tag{S1e}$$

Thus, chirped pulses are longer and weaker, but the product $\mathcal{A}_\beta{}^2 T_\beta$ is constant, i. e., the energy of the pulse does not depend on the chirp β. This is just a manifestation of Parseval's theorem: Since we do not change the absolute value in the frequency domain, but just the phase as in Eq. (S1b), the integral of the absolute square in the time domain is also unchanged.

Throughout the text we will use the dimension-less quantity β in order to characterize the chirp of the pulse.

2 Time-dependent Schrödinger equation

2.1 Basis-set representation

We will discuss the time evolution of the electron state $\psi(t)$ due to the Hamiltonian $\hat{H}(t) = \hat{H}_0 + \mathcal{A}_\beta(t)\,\hat{p}$ in terms of a field-free basis $\hat{H}_0\varphi_j = E_j\varphi_j$. For

$$\psi(t) = \sum_j \mathrm{e}^{\mathrm{i}\chi_j}\varphi_j a_j(t) \quad \text{and} \quad V_{jj'} = \mathrm{e}^{-\mathrm{i}[\chi_j-\chi_{j'}]}\langle\varphi_j|\hat{p}|\varphi_{j'}\rangle. \tag{S2}$$

the time-dependent Schrödinger equation (TDSE) reads

$$\mathrm{i}\,\dot{a}_j(t) = \sum_{j'} \left[E_j\delta_{jj'} + \mathcal{A}_\beta(t)\,V_{jj'}\right] a_{j'}(t). \tag{S3}$$

This description applies for both cases discussed in the text, the 1D model system and the 3D case of helium. The additional phase factors in the expansion (S2) allow for working with real Hamilton matrices. We chose $\chi_j = (-1)^j\pi/4$ and $\chi_j = (-1)^{\ell_j}\pi/4$ for the 1D and 3D case, respectively. In the 1D case j is odd/even for a gerade/ungerade state φ_j, in the 3D case ℓ_j is the angular momentum of the field-free state φ_j.

2.2 Two-level system and rapid adiabatic passage

For a two-level system we use

$$c_0(t) \equiv \mathrm{e}^{\mathrm{i}[E_0 t - \phi_\beta(t) + E_1 t]/2} a_0(t),\ c_1(t) \equiv \mathrm{e}^{\mathrm{i}[E_0 t + \phi_\beta(t) + E_1 t]/2} a_1(t) \tag{S4}$$

to get instead of (S3)

$$\mathrm{i}\begin{pmatrix}\dot{c}_0(t)\\ \dot{c}_1(t)\end{pmatrix} = \begin{pmatrix}+\frac{1}{2}\Delta_\beta(t) & \frac{1}{2}\Omega_{01}(t)\\ \frac{1}{2}\Omega_{10}(t) & -\frac{1}{2}\Delta_\beta(t)\end{pmatrix}\begin{pmatrix}c_0(t)\\ c_1(t)\end{pmatrix}, \tag{S5}$$

with the Rabi frequency and the detuning

$$\Omega_{jj'}(t) \equiv \mathcal{A}_\beta\, g_\beta(t)\, V_{jj'}, \qquad \Delta_\beta(t) = E_0 + \omega_\beta(t) - E_1. \tag{S6}$$

Hereby we have used the time-dependent frequency (S1d) and simplified the coupling by means of the rotating-wave approximation, i. e. replaced $\cos\big(\phi(t)\big)$ by either $\frac{1}{2}\mathrm{e}^{+\mathrm{i}\phi(t)}$ or $\frac{1}{2}\mathrm{e}^{-\mathrm{i}\phi(t)}$.

The TDSE (S5) describes the process of rapid adiabatic passage [2]. Hereby one transfer the population from one state to the other by adiabatically changing the character of eigenstate including the non-diagonal coupling terms.

2.3 Dressed-state description

Similar to Eq. (S4) one can split the amplitudes $a_j(t)$ into a sum as

$$a_j(t) = \sum_k c_{jk}(t)\mathrm{e}^{\mathrm{i}k\phi_\beta(t)}, \tag{S7}$$

which results in a partitioned TDSE

$$\mathrm{i}\,\dot{c}_{jk}(t) = \big[E_j + k\,\omega_\beta(t)\big]\,c_{jk}(t) + \sum_{k'=k\pm1}\sum_{j'}\Omega_{jj'}(t)\,c_{j'k'}(t) \tag{S8a}$$

$$\text{with}\quad \Omega_{jj'}(t) \equiv \frac{\mathcal{A}_\beta}{2} g_\beta(t)\,V_{jj'}. \tag{S8b}$$

In principle the sum over k runs from $-\infty$ to $+\infty$, but one can limit it to finite values. The coupling matrix $\Omega_{jj'}$ is proportional to the envelope g_β of the pulse (S1), the oscillations are transferred to the diagonal blocks. It has only finite values for states that are coupled: For the 1D model discussed in the text this requires that (i) one of states is gerade and the other one is ungerade and (ii) the "photon-number" difference should be $|k-k'| = 1$.

2.3 Numerical propagation

The TDSEs for both, the 1D model system and the 3D helium atom, are propagated in terms of field-free eigenstates. Therefore, eigenenergies and eigenfunctions as well the corresponding

dipole matrix elements are calculated numerically. For the 1D model we considered the lowest 200 states in a box of size $x = -250\,\mathrm{a_0} \ldots +250\,\mathrm{a_0}$ (with $\mathrm{a_0}$ being the Bohr radius) and used a Numerov approach with a step size of $\delta x = 0.1\,\mathrm{a_0}$. For the 3D helium atom we use an effective potential [3]. For angular momenta $\ell = 0 \ldots 4$ we calculated the lowest 750 states in a box of size $r = 0 \ldots 10^3 \mathrm{a_0}$ with a Numerov step size of $\delta r = 0.01\,\mathrm{a_0}$. For the longer pulses shown in Fig. 5 of the main text we used 2250 states with $r_{\max} = 3{\times}10^3\,\mathrm{a_0}$ (for $T > 4\,\mathrm{fs}$) and 3750 states with $r_{\max} = 5{\times}10^3\,\mathrm{a_0}$ (for $T > 12\,\mathrm{fs}$), respectively.

3 Suppression of ionization

3.1 Dressed-state description

In order to understand the ionization dynamics it is sufficient to consider a set of essential states, which consist of the ground state (E_0), the excited state (E_1), and a gerade (E_g) and an ungerade (E_u) continuum state, respectively. Those states, in its original and dressed form, build this effective Hamilton matrix

$$H_\mathrm{eff}(t) = \left(\begin{array}{cccc:cccc:cc}
\overline{E}_0{+}2\omega & \Omega_{01} & 0 & 0 & 0 & 0 & 0 & \Omega_{0\mathrm{u}} \\
\Omega_{10} & \widetilde{E}_1{+}\omega & 0 & 0 & \Omega_{1\mathrm{g}} & 0 & 0 & 0 \\
0 & 0 & \overline{E}_\mathrm{g}{+}\omega & 0 & 0 & \Omega_{\mathrm{gu}} & 0 & 0 \\
0 & 0 & 0 & \widetilde{E}_\mathrm{u}{+}\omega & \Omega_{\mathrm{ug}} & 0 & 0 & 0 \\ \hdashline
0 & \Omega_{\mathrm{g}1} & 0 & \Omega_{\mathrm{gu}} & \overline{E}_\mathrm{g} & 0 & 0 & \Omega_{\mathrm{gu}} \\
0 & 0 & \Omega_{\mathrm{ug}} & 0 & 0 & \widetilde{E}_\mathrm{u} & \Omega_{\mathrm{ug}} & 0 \\ \hdashline
0 & 0 & 0 & 0 & 0 & \Omega_{\mathrm{gu}} & \overline{E}_\mathrm{g}{-}\omega & 0 \\
\Omega_{\mathrm{u}0} & 0 & 0 & 0 & \Omega_{\mathrm{ug}} & 0 & 0 & \widetilde{E}_\mathrm{u}{-}\omega
\end{array}\right). \tag{S9}$$

Hereby, we use the abbreviation $\omega \equiv \omega_\beta(t)$, omit the time argument for all Ω, mark gerade and ungerade state with a bar or a tilde, respectively, and separate blocks with a definite photon number k by dashed lines. The two continuum energies are the same: $E = \overline{E}_\mathrm{g} = \widetilde{E}_\mathrm{u}$. Note the the couplings Ω_{ug} between the two continuum state are much larger than among bound states (Ω_{01}) or between bound and continuum states ($\Omega_{0\mathrm{g}}$ and $\Omega_{1\mathrm{u}}$). That is the reason that continuum states dressed by ± 1 photons have to be included in the effective Hamilton matrix (S9).

In order to understand the emerging dynamics from matrix (S9), one should rearrange it by exchanging columns and rows to get

$$H_\mathrm{eff}(t) = \left(\begin{array}{cc:ccc:ccc}
\overline{E}_0{+}2\omega & \Omega_{01} & \Omega_{0\mathrm{u}} & 0 & 0 & 0 & 0 & 0 \\
\Omega_{10} & \widetilde{E}_1{+}\omega & 0 & \Omega_{1\mathrm{g}} & 0 & 0 & 0 & 0 \\ \hdashline
\Omega_{\mathrm{u}0} & 0 & \widetilde{E}_\mathrm{u}{-}\omega & \Omega_{\mathrm{ug}} & 0 & 0 & 0 & 0 \\
0 & \Omega_{\mathrm{g}1} & \Omega_{\mathrm{gu}} & \overline{E}_\mathrm{g} & \Omega_{\mathrm{gu}} & 0 & 0 & 0 \\
0 & 0 & 0 & \Omega_{\mathrm{ug}} & \widetilde{E}_\mathrm{u}{+}\omega & 0 & 0 & 0 \\ \hdashline
0 & 0 & 0 & 0 & 0 & \overline{E}_\mathrm{g}{-}\omega & \Omega_{\mathrm{gu}} & 0 \\
0 & 0 & 0 & 0 & 0 & \Omega_{\mathrm{ug}} & \widetilde{E}_\mathrm{u} & \Omega_{\mathrm{ug}} \\
0 & 0 & 0 & 0 & 0 & 0 & \Omega_{\mathrm{gu}} & \overline{E}_\mathrm{g}{+}\omega
\end{array}\right). \tag{S10}$$

Thereby we end up with three blocks: one consisting of bound states only and two decoupled blocks in the continuum. Only one of the two is connected to the bound-state block, the other one (at the bottom-right) is not and therefore can be neglected from now on.

In order to understand the chirp-dependent ionization dynamics we have to consider the four top-left blocks, which are given also in the text. In the diagonal, not only the 2×2 bound-state block, but also the 3×3 continuum-state block can be diagonalized analytically to get

$$H_{\mathrm{eff}}(t) = \begin{pmatrix} E_\downarrow & 0 & \cdot & C_\downarrow & \cdot & \cdot & \cdot & \cdot \\ 0 & E_\uparrow & \cdot & C_\uparrow & \cdot & \cdot & \cdot & \cdot \\ \cdot & \cdot & \cdot & 0 & \cdot & \cdot & \cdot & \cdot \\ C_\downarrow & C_\uparrow & 0 & E & 0 & \cdot & \cdot & \cdot \\ \cdot & \cdot & \cdot & 0 & \cdot & \cdot & \cdot & \cdot \\ \cdot & \cdot & \cdot & \cdot & \cdot & \cdot & \cdot & \cdot \\ \cdot & \cdot & \cdot & \cdot & \cdot & \cdot & \cdot & \cdot \\ \cdot & \cdot & \cdot & \cdot & \cdot & \cdot & \cdot & \cdot \end{pmatrix}, \tag{S11}$$

whereby matrix entries with a dot are not specified (they are not necessarily 0), since they are not relevant for the following discussion. The respective eigenvectors are

$$V_{\downarrow\uparrow} = \frac{1}{\sqrt{2}}(1, \pm 1) \qquad \text{and} \qquad \widetilde{V} = \frac{1}{\sqrt{2{\Omega_{\mathrm{ug}}}^2 + \omega^2}}\big(-\Omega_{\mathrm{ug}}, \omega, +\Omega_{\mathrm{ug}}\big). \tag{S12}$$

Relevant are the two matrix elements connecting either of the adiabatic states with energy $E_{\downarrow\uparrow}$ with the continuum state at energy E. They read explicitly

$$C_{\downarrow\uparrow} = \frac{\mp\Omega_{0\mathrm{u}}\Omega_{\mathrm{ug}} - \omega\Omega_{1\mathrm{g}}}{\sqrt{2\omega^2 + 4{\Omega_{\mathrm{ug}}}^2}} \tag{S13}$$

and are given as Eq. (3) in the main text. Apparently, under the condition $\Omega_{0\mathrm{u}}\Omega_{\mathrm{ug}} = \omega\Omega_{1\mathrm{g}}$ the two couplings $C_{\downarrow\uparrow}$ may have very different absolute values.

3.2 Strong-field propagated wavefunction

The Volkov propagator [see Eq. (5c) in the main text]

$$\hat{U}(t,t') = \mathrm{e}^{-\mathrm{i}\int_{t'}^{t}\mathrm{d}t''[\hat{p}^2/2 + \hat{p}\,\mathcal{A}_\beta\cos(\omega_0 t'')]} \tag{S14}$$

is diagonal in the momentum representation

$$\big\langle k|\hat{U}(t,t')|k\big\rangle = \mathrm{e}^{-\mathrm{i}\int_{t'}^{t}\mathrm{d}t''[k^2/2 + \mathcal{A}_\beta k\cos(\omega_0 t'')]} = \mathrm{e}^{-\mathrm{i}[S(t) - k^2 t'/2 - \lambda\sin(\omega_0 t')]}, \tag{S15}$$

with $\lambda \equiv \mathcal{A}_\beta k/\omega_0$ being the electron-photon coupling parameter and $S(t) \equiv k^2 t/2 + \lambda\sin(\omega_0 t)$ accounting for a phase which is irrelevant for the absolute value of the amplitude (S15). By means of the Jacobi-Anger expansion the diagonal form of $\hat{U}$ reads

$$\big\langle k|U(t,t')|k\big\rangle = \mathrm{e}^{-\mathrm{i}S(t)}\sum_{m=-\infty}^{+\infty}\mathrm{e}^{\mathrm{i}[k^2/2 + m\omega_0]t'}J_m(\lambda). \tag{S16}$$

Inserting this into Eq. (5a) of the main text we get

$$\big\langle k|\psi(t\to\infty)\big\rangle = -\mathrm{i}\,\mathrm{e}^{\mathrm{i}S(t)}\lambda\omega_0 T_\beta\frac{\sqrt{\pi}}{2}\sum_m \mathrm{e}^{-\left[k^2/2 - [m+2]\omega_0 - E_0\right]^2 {T_\beta}^2} \times \big[\mathrm{sign}(\beta)J_{m+1}(\lambda)\langle k|0\rangle + J_m(\lambda)\langle k|1\rangle\big]. \tag{S17}$$

The dominant ionization channel is the two-photon absorption, collapsing the the sum in (S17) to the term $m = 0$, with the final continuum energy $k^2/2 = E_0 + 2\omega_0$. Since the argument in the Bessel function is $\lambda \lesssim 1$, the term with $m = 0$ dominates. This allows for additionally retaining only the lowest order of λ in the Bessel functions $J_0(\lambda) = 1 + \mathcal{O}(\lambda^2)$ and $J_1(\lambda) = \lambda/2 + \mathcal{O}(\lambda^3)$. Thus we may formulate the condition for ionization suppression as

$$\frac{\lambda}{2}\langle k|0\rangle = \langle k|1\rangle \qquad \text{or} \qquad \frac{\mathcal{A}_\beta}{2}\frac{\langle k|0\rangle}{\langle k|1\rangle} = \frac{\omega_0}{k}, \tag{S18}$$

where we have used in the latter version the explicit expression of the electron-photon coupling parameter λ, cf. its definition (6) in the main text. The condition for continuum suppression obtained from the dressed-state picture [Eq. (4) in the main text] and from the strong-field amplitude with a locked initial state [Eq. (S18) above] are equivalent. It can be shown that for large-k continuum states $V_{\mathrm{ug}} = \frac{2}{\pi}k$ and $\sum_{j\in \mathrm{u}} V_{j\mathrm{g}} = k$, where the sum corresponds to the Volkov-propagated state.

4 Pulses "flipped" in time

We will proof that the final occupation of an initially populated state is the same in both cases, when the system is driven either by a pulse $F(t)$ or its "flipped" version $\widetilde{F}(t) \equiv F(-t)$. In other words the depletion of the initial state does not depend on the "direction" (i. e. in the cases studied in the text it does not depend on the sign of chirp) of the driving pulses.

Instead of looking at the TDSE (S3) it is convenient to consider the time-evolution operator $\hat{U}(t, t')$, which is also defined by a "TDSE", which reads in a basis or close-coupling representation

$$\mathrm{i}\frac{\partial}{\partial t}\boldsymbol{\mathcal{U}}(t, t') = \boldsymbol{\mathcal{H}}(t)\,\boldsymbol{\mathcal{U}}(t, t') \tag{S19}$$

with bold symbols denoting matrices and the Hamilton matrix in particular being $\boldsymbol{\mathcal{H}}(t) = H_{jj'}(t) = E_j\delta_{jj'} + F_\beta(t)\,V_{jj'}$ as in Eq. (S3). The formal solutions of (S19) read for both cases, i. e. driving by $F(t)$ and $\widetilde{F}(t)$, respectively,

$$\boldsymbol{\mathcal{U}}(+\tau, -\tau) = \mathrm{e}^{-\mathrm{i}\,\delta t\,\boldsymbol{\mathcal{H}}(t_n)} \ldots \mathrm{e}^{-\mathrm{i}\,\delta t\,\boldsymbol{\mathcal{H}}(t_1)}, \tag{S20a}$$

$$\widetilde{\boldsymbol{\mathcal{U}}}(+\tau, -\tau) = \mathrm{e}^{-\mathrm{i}\,\delta t\,\boldsymbol{\mathcal{H}}(t_1)} \ldots \mathrm{e}^{-\mathrm{i}\,\delta t\,\boldsymbol{\mathcal{H}}(t_n)}, \tag{S20b}$$

whereby we consider $n \to \infty$, $\delta t \to 0$, $n \times \delta t = 2\tau$, and $t_k = -\tau + [2k-1]\delta t$. By means of $\boldsymbol{\mathcal{H}}(t_k) = \boldsymbol{\mathcal{H}}^\top(t_k)$ one can deduce from the two sums (S20)

$$\widetilde{\boldsymbol{\mathcal{U}}}(+\tau, -\tau) = \boldsymbol{\mathcal{U}}^\top(+\tau, -\tau) \qquad \text{i. e.} \qquad \widetilde{\mathcal{U}}_{jj'}(+\tau, -\tau) = \mathcal{U}_{j'j}(+\tau, -\tau). \tag{S21}$$

In particular the special case $\widetilde{\mathcal{U}}_{jj}(+\tau, -\tau) = \mathcal{U}_{jj}(+\tau, -\tau)$ is interesting, since it guarantees that from $a_j(-\tau) = \widetilde{a}_j(-\tau) = \delta_{jj_{\mathrm{init}}}$ follows immediately $a_{j_{\mathrm{init}}}(+\tau) = \widetilde{a}_{j_{\mathrm{init}}}(+\tau)$ with τ being arbitrarily large. So indeed, the amplitudes of the initial state j_{init} are the same, irrespective of the "direction" of the pulse.

References

[1] M. Wollenhaupt, A. Assion, and Th. Baumert, in *Springer Handbook of Lasers and Optics*, chapter "Short and Ultrashort Laser Pulses", Springer Berlin Heidelberg (2012).

[2] N. V. Vitanov, T. Halfmann, B. W. Shore, and K. Bergmann, *Laser-induced population transfer by adiabatic passage techniques*. Annu. Rev. Phys. Chem. **52**, 763 (2001).

[3] X. M. Tong and C. D. Lin, *Empirical formula for static field ionization rates of atoms and molecules by lasers in the barrier-suppression regime*. J. Phys. B **38**, 2593 (2005).